Modeling Nanoparticle−Alveolar Epithelial Cell Interactions under Breathing Conditions Using Captive Bubble Surfactometry

David Schürch,[†,‡] Dimitri Vanhecke,[†] Martin J. D. Clift,[†] David Raemy,[†,‡] Dorleta Jimenez de Aberasturi,[§] Wolfgang J. Parak,[§] Peter Gehr,[‡] Alke Petri-Fink,[†] and Barbara Rothen-Rutishauser*,[†,‖]

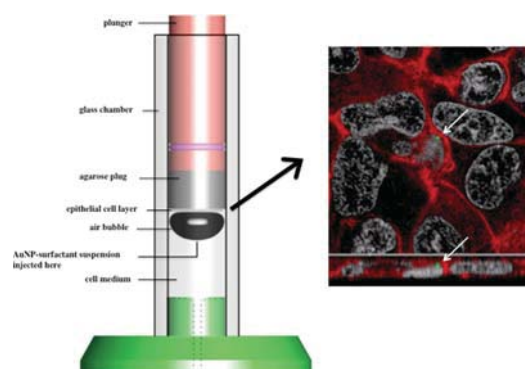[†]Adolphe Merkle Institute, University of Fribourg, Fribourg, Switzerland
[‡]Institute of Anatomy, University of Bern, Bern, Switzerland
[§]Fachbereich Physik, Philipps Universität Marburg, Marburg, Germany
[‖]Respiratory Medicine, Bern University Hospital, Bern, Switzerland

ⓢ *Supporting Information*

ABSTRACT: Many advances have been made in recent years in cell culture models of the epithelial barrier of the lung from simple monolayers to complex 3-D systems employing different cell types. However, the vast majority of these models still present a static air−liquid interface which is unrealistic given the dynamic nature of breathing. We present here a method where epithelial lung cells are integrated into a system, the captive bubble surfactometer, which allows the cyclical compression and expansion of the surfactant film at the air−liquid interface, thus modeling the dynamics of breathing. We found that cellular uptake of deposited gold nanoparticles was significantly increased under the dynamic (breathing) conditions of compression and expansion as compared to static conditions. The method could be very useful for studying nanoparticle−alveolar lung cell interactions under breathing conditions for applications in nano-medicine and toxicology.

INTRODUCTION

With every breath, millions of airborne particles enter the human respiratory system. Following inhalation, these particles deposit in the different regions of the respiratory tract in a size-dependent manner.[1,2] Larger particles (1−10 μm) preferentially deposit in larger conducting airways (i.e., trachea and bronchi), whereas smaller particles (i.e., nanoparticles (NPs, <100 nm)) localize to more peripheral lung regions (i.e., alveoli).[3] NPs, in particular, can be released into the environment from combustion-derived processes and also from the production and use of engineered NPs found in a variety of consumer products. Besides the geometry of the airways and breathing pattern, the specific NP size and chemical composition are important factors with regard to their deposition and clearance from the respiratory tract. Once deposited, NPs interact with various structural barriers such as the pulmonary surfactant film at the air−liquid interface and are displaced via wetting forces into the aqueous hypophase.[4] As a result of this displacement, NPs come into contact with more than 40 different cell types in the respiratory tract. These cell types comprise of epithelial and endothelial cells, fibroblasts, nerve cells, and lymphoid cells as well as immune cells such as macrophages and dendritic cells.[5] The epithelium is "the" primary cellular barrier endowed with tight junctions whose effectiveness is greatly enhanced by the aqueous surface lining layer and the mucociliary escalator.[6]

In recent years, scientists have attempted to take advantage of deposition characteristics of NPs in the lungs, e.g., in the field of drug delivery. The alveolar surface of the lung presents a very attractive target for local and systemic delivery of NP-drug carriers primarily due to its large surface area, thin air-blood barrier, and lack of first-pass metabolic activity. These unique characteristics make rapid therapeutic effects possible, at the lung itself and throughout the body, with a potentially high bioavailability.[7,8]

To assess the potential therapeutic value and safety of such materials, there is a need for the development of cost-effective *in vitro* models mimicking the alveolar epithelial barrier of the human lung. Cellular models of this interface have advanced in recent years, beyond simple monolayer systems to 3-D models employing different cell types.[9] In addition, animal models often do not accurately predict possible reactions in human lungs due to species differences. Unfortunately, the vast majority of these human cell culture models cannot adequately mimic the specific composition and mechanics of the alveolar surface. In particular, they typically present a static air−liquid interface, which is clearly unrealistic given the cyclical motion of the alveolar surface during breathing. A recent exception is
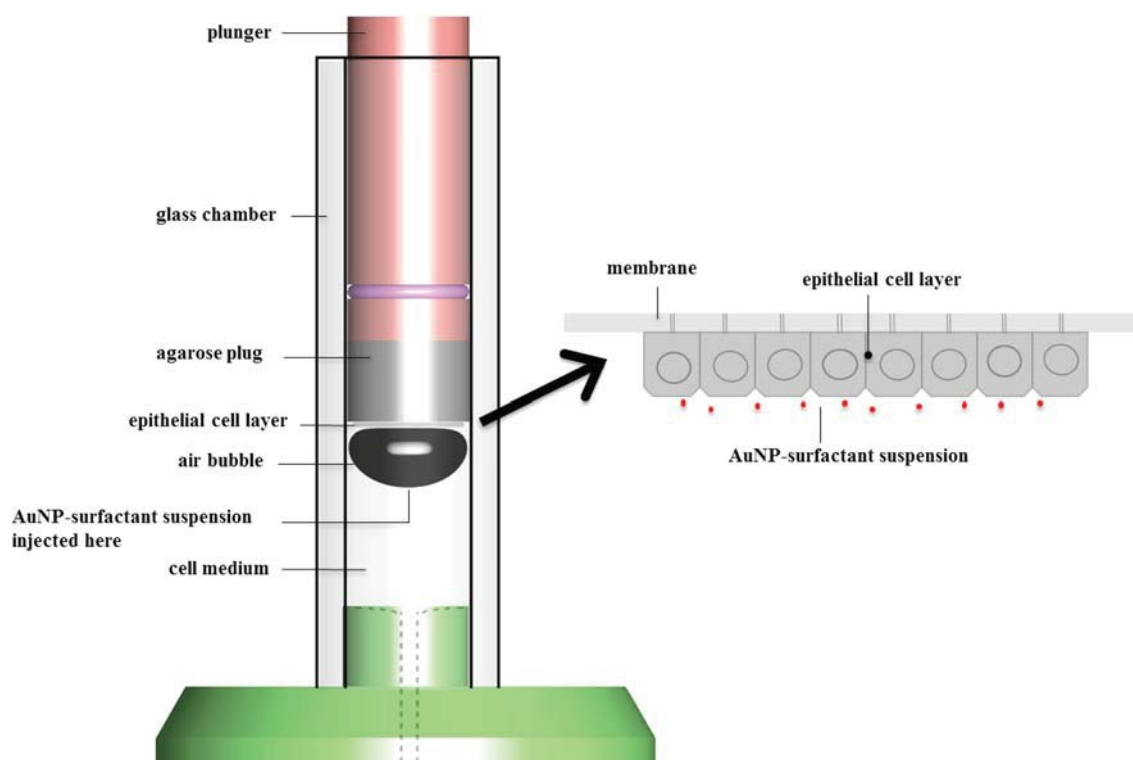
Figure 1. Experimental setup for the captive bubble surfactometer (CBS)-cell method. Displayed on the left is the CBS chamber: the bubble rests on a monolayer of epithelial cells, making an air−liquid-cellular interface, rather than directly on the agarose substrate as in the standard CBS setup. Right: schematic diagram of air−liquid−cellular interface. Gold nanoparticles (Au-NPs) in suspension with surfactant are injected directly at the air−liquid interface; thus, the surfactant film is in close proximity to the surface of the cell layer.

provided by Huh et al.,[10] whose lung on a chip model features mechanical stretching of an interface combining alveolar epithelial and microvascular endothelial cells, to simulate the dynamics of breathing. This system has also been used to model disease states of the human lung such as pulmonary edema.[11]

Since the surfactant film lining the alveoli is the first point of contact for NPs inhaled into the deep lung,[12] a model with a more realistic surface film in terms of composition and dynamics could be important for studying NP−surfactant and NP−cell interaction. Indeed, the surfactant film likely promotes the displacement of air deposited particles toward the epithelium in airways and alveoli, with displacement enhanced at low surface tensions.[13] Therefore, the addition of surfactant in any *in vitro* study has to be strongly considered. Such consideration has recently been highly recommended for all *in vitro* lung research.[14]

Here we present a method that addresses the limitation of a static interface inherent in the vast majority of *in vitro* models of the epithelial barrier. We have integrated cultured epithelial lung cells into a device, the captive bubble surfactometer (CBS), which effectively models surfactant film dynamics of the air−liquid interface.[15,16] In the method, the surfactant film at the air−liquid interface of cultured epithelial lung cells can be compressed and expanded to give changes in surface tension similar to those that occur during breathing, as concluded from the direct measurement of surface tension in excised animal lungs,[17,18] thus adding a new mechanistic dimension to typical static cell culture models.

For this study, we integrated a monolayer of alveolar epithelial type II cells, i.e., the A549 cell line[19] which has been shown to produce and release surfactant when exposed to air

for 24 h,[20] into the CBS device in such a way that cell viability was maintained under experimental conditions. Subsequently, we investigated the influence of a dynamic interface, i.e., compressed and expanded, on interaction and uptake (by the underlying epithelial cells) of fluorescently labeled gold nanoparticles (Au-NPs) which have been shown in other studies to be sufficiently biocompatible. Thus, we applied surfactant containing these Au-NPs to the air−liquid interface of the A549 epithelial cells, subjected the interface to dynamic or static conditions, and then analyzed the cell layer and the intracellular Au-NPs by laser scanning microscopy (LSM).

■ MATERIALS AND METHODS

CBS-Cell Method and Experiments. All CBS-cell experiments were carried out in a computer-controlled CBS based on the apparatus described by Schoel et al. in 1994.[16] The schematic diagram in Figure 1 depicts the CBS chamber as used for the CBS-cell experiments.

Cell Insertion into CBS. The cell culture insert covered with a monolayer of A549 cells was removed from its well plate and placed on a Teflon block where a disk of approximately 1 cm diameter was cut out utilizing a hollow cylinder finely sharpened around the edges. The membrane disk containing the cells was carefully removed from the block with tweezers and placed on top of an agarose substrate plug, where it adhered strongly due to cohesive forces. The agarose plug and cells were subsequently inserted into the glass CBS chamber, and the chamber filled with approximately 1.5 mL of RPMI 1640 cell culture medium (w/25 mM Hepes, LabForce AG Nunningen, Switzerland) kept at 37 °C. The chamber was immediately installed in the CBS apparatus, with temperature control set at 37 °C, and closed with a screw-on cap. The chamber solution was degassed by applying negative pressure for 5 min and then opening the screw cap to expel accumulated gas. An air bubble of 6 mm diameter was injected into the chamber where it came to rest against the agarose substrate. A measured amount (0.01 μL) of Curosurf surfactant (Curosurf 120, 80
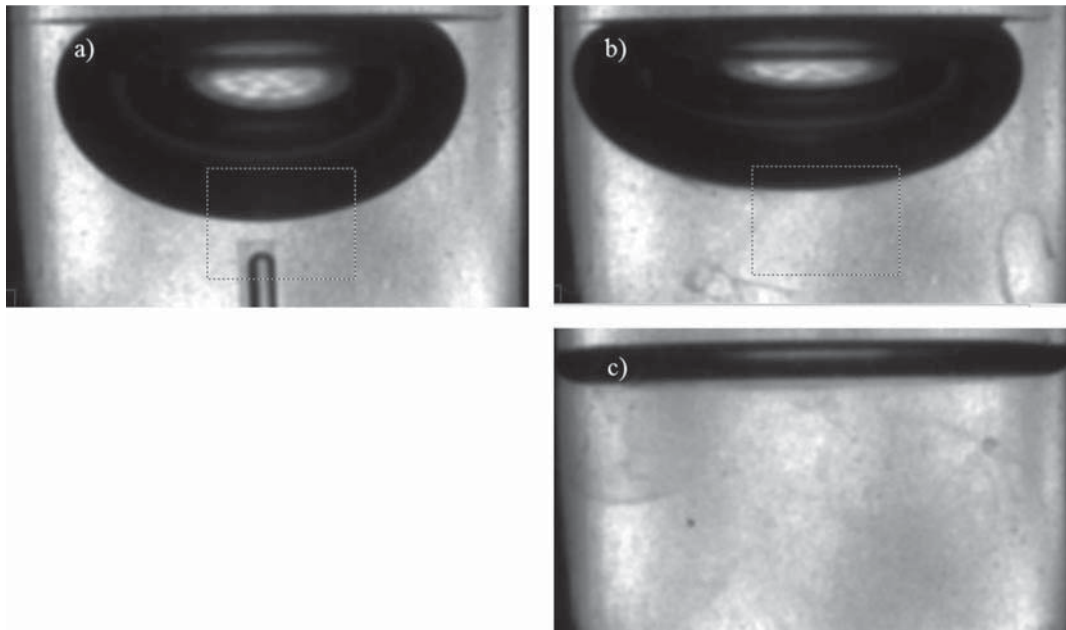
Figure 2. Photos of air−liquid−cellular interface during the CBS-cell method protocol, 20× magnification. (a) Before application of Au−NP−surfactant suspension via microtube. The interfacial surface tension is approximately 45 mN/m, significantly lower than for a pure air−water interface, likely due to surfactant secreted by the epithelial cells. (b) 5 min after directly injecting Au−NP−surfactant suspension. The surface tension of the interfacial film has reached an equilibrium value near 25 mN/m. (c) Interfacial film at maximum compression and minimum surface tension, approximately 1 mN/m, reached during dynamic cycling.

mg/mL Phospholipid fraction, Chiesi, Parma, Italy) diluted to 20 mg/mL phospholipids, containing Au-NPs at either 28 or 40 nM, was injected directly at the air−liquid−cellular interface using a micro-syringe, with a 30 gauge needle and an attached Teflon microtube of an inner diameter of 0.03 mm. For experiments under dynamic conditions, the interfacial film was allowed to equilibrate for 2 min, after which time the film was compressed and expanded continuously at a rate of 20 cycles/min by increasing or decreasing the pressure inside the glass chamber via motor driven plunger (Figure 1; for a movie file please see Supporting Information). Under static conditions, the film was not compressed or expanded but simply left alone for the duration of the experiment (25 min). After this time, the CBS chamber was removed from the apparatus and the cell layer, still inside of the chamber, was rinsed several times with fresh medium (Rosewell Park Memorial Institute (RPMI) 1640). Next, the agarose plug and adhered membrane (cell layer) were removed from the chamber, and the membrane was carefully peeled off with tweezers and placed in a previously prepared solution of 3% paraformaldehyde (PFA) for 12 min to fix the cells. The membrane containing the fixed cell layer was then placed in a solution of 0.1 M glycine (Sigma-Aldrich, Buchs, Switzerland) and stored at 4 °C for later staining.

All bubbles were imaged (see examples in Figure 2) utilizing a video camera (Pulnix TM 7 CN) and video capture software. For all imaged bubbles, the volume, area, and surface tension were calculated using the measured height and diameter of the bubble according to the method established by Schoel et al.[16]

Cell Culture. The A549 cell line[19] was purchased from American Tissue Type Culture Collection (LGC Promochem, Molsheim, France). Cells were cultured in RPMI 1640 medium supplemented with 10% fetal calf serum (FCS), 1% L-glutamine, and 1% pennicillin/streptomycin (GIBCO, Switzerland) and grown in 6-well plates (BD Falcon 6-well tissue culture plate, BD Biosciences, Allschwil Switzerland) on cell-culture transwell insert (BD Falcon, poly(ethylene terephthalate) (PET) membranes, 4.2 cm², with 3 μm pores (Allschwil Switzerland)) as described previously in more detail.[9] The cells were cultured for 7 days until forming a confluent, tight layer with cell growth reaching a plateau. The medium was changed twice a week, and exposures were performed on day 7.

Cell Viability Assessment (Live/Dead Staining). Apoptotic and necrotic cells of the A549 cell layers were made visible using the Annexin-V-FLUOS Staining Kit (Roche Diagnostics, Schweiz AG). Briefly, the two dyes, Annexin V fluorescein and propidium iodide, were diluted together in phosphate-buffered saline (PBS, 50:1 v/v) and added dropwise to the cell layer surface assuring complete coverage. The cells with added dyes were incubated for 10 min and rinsed with PBS. They were then mounted on a microscope slide and visualized by a Leica DMI 4000B fluorescence microscope using filter cube settings FITC and Cy3 for excitation and detection of the fluorescein and propidium iodide dyes, respectively, and a 20× (multi-immersion, NA 0.7) objective. Pictures were taken with a Leica DFC 350 FX, cooled fluorescence black and white camera, in a uniform random sampling mode, generating at least five different pictures per cell layer. For control samples, a square (approximately 2 cm²) was cut from the cell layer with a razor and immediately stained and imaged. To gauge the number of cells typically contained within a given area, they were treated with 3% paraformaldehyde (PFA) (Sigma-Aldrich Chemie GmbH, Buchs, Switzerland) for 10 min (fixing all the cells present) and then stained and imaged as above.

Nanoparticles. Fluorescently labeled Au-NPs were prepared in aqueous suspension at a concentration of 55 nM. They consisted of a Au core, in the range of 5 nm diameter, coated with a poly(methacrylic acid) (PMA) polymer shell containing the fluorophore ATTO 590 (Au-PMA-ATTO 2%). The synthesis of the fluorescent polymer, the synthesis of the Au NPs, and their coating with the polymer (in which 2% of the anhydride rings were linked with ATTO 590) as well as the characterization of the resulting NPs have been previously detailed.[22,23]

Au−NP−Surfactant Suspensions. Experiments were carried out with suspensions containing two different concentrations of Au-NPs, prepared as follows: Au-NPs (aqueous suspension, 55 nM) were mixed with diluted (40 mg/mL phospholipid) or undiluted surfactant (Curosurf 120, 80 mg/mL phospholipid fraction, Chiesi, Parma, Italy) at a ratio of 1:1 or 3:1 (v/v), resulting in Au-NP concentrations of approximately 28 and 40 nM, respectively, and a surfactant phospholipid concentration of 20 mg/mL. The mixtures were vortexed for 30 s, incubated at 37 °C for 15 min, and vortexed again just before usage.

Transmission Electron Microscopy (TEM) measurements of Au−NP−Surfactant Suspensions. Probes were prepared by placing a small drop of Au−NP−surfactant suspension on the TEM substrate and then removing most of the drop with a piece of filter paper, thereby leaving only a thin film covering the substrate. The film-coated substrate was slowly dried over several hours and then imaged. Images were taken with a HITACHI H-1700 TEM at resolutions of 1.9 and 0.4 nm/pixel for primary magnifications of 20K× and 100K×, respectively.

Imaging and Quantitation of Intracellular Au-NPs with LSM. For LSM analysis, insert membranes with the cells were fixed with 3% PFA and stained with DAPI (Sigma-Aldrich Chemie GmbH, Buchs, Switzerland) and Alexa 488 Phalloidin (Invitrogen, Basel, Switzerland) as described previously.[9] Fluorescently labeled Au-NPs in the A549 cell layers were imaged and quantified with a Zeiss 710 confocal microscope.

The confocal 3D stacks (Z-stacks) were recorded using a plan-apochromat 63×/NA = 1.40 lens. The three channels (DAPI, ex = 405 nm; Phalloidin-Alexa 488, ex = 488 nm, and the ATTO 590 fluorochrome, ex = 561 nm) were line averaged four times to ensure a high signal-to-noise ratio. 3D images were constructed from the recorded optical sections using Imaris software (Bitplane AG, Zürich, Switzerland).

For Au-NP quantitation, in each sample, five systematic random sampled stitched panels (each composed of 5 × 5 images with a total size of 650 by 650 μm) were recorded on the above-mentioned microscope equipped with a 40×/NA = 0.9 objective lens at a theoretical pixel size of 0.127 μm. In order to avoid out of focus particles, the pinhole was opened to 8.4 μm. The ATTO 590 fluorophore was excited using a 561 nm HeNe laser, and the resulting emitted signal was separated using the main beam splitter (MBS) 561/488 nm long pass beam splitter. The presence of Au-NPs in the resulting images was assessed by an impartial expert not involved in the CBS experiment. Arguments for evaluating an event as an Au-NP were the signal (a localized, high fluorescence signal) combined with morphology (a clearly delineated edge) and size (approximately less than 1 μm diameter). In case of doubt, the event was not counted as a particle event. Please note that due to the limited lateral resolution of the LSM, no single NPs could be observed, and particle events typically may comprise several NPs in close distances, such as for example for NPs inside the same endosomal/lysosomal vesicles.[24]

Statistical Analysis. Results, unless stated otherwise, are based on mean values ± standard deviation (SD), averaged from at least four independent experiments. To determine statistical significance, the 2-tailed t test was applied with a significance level of 0.05.

RESULTS

Size Distribution of Au-NPs in Surfactant As Determined by TEM. Figure 3 shows a representative TEM image of the higher concentration Au-NP surfactant suspension (40 nM) used in the study. There appears to be little, if any, agglomeration. The diameter of the majority of the particles measured 4−6 nm, in the range expected for these particular Au-NPs.[22]

Biophysical Characterization of Lung Surfactant with Added Au-NPs in CBS. Figure 4 depicts the results of a surface activity assessment in the CBS-cell method based on the biophysical markers of adsorption kinetics, postexpansion adsorption kinetics, and dynamic compression/expansion isotherms. The results are representative (see Supporting Information Table S1) for experiments where we injected surfactant containing Au-NPs directly at the air−liquid−cellular interface.

Adsorption Kinetics. In the lung, extremely fast adsorption of surfactant secreted to the air−liquid interface is vital for the initial formation and maintenance of a surface tension lowering film.[25] In the CBS method the surface tension drops
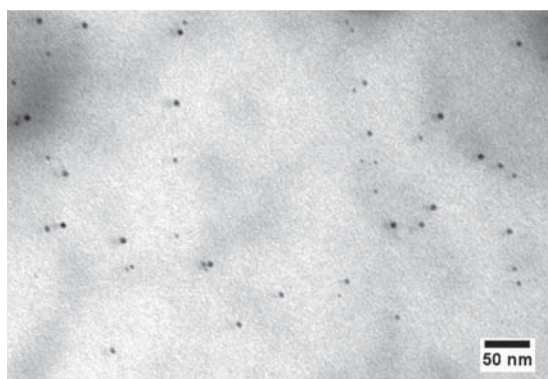

Figure 3. Visualization of Au−NP−surfactant suspension with TEM (magnification 100K×). Agglomeration in the surfactant matrix appears minimal. Particle concentration was approximately 40 nM in surfactant containing 20 mg/mL phopholipids.

immediately and typically reaches equilibrium values near 25 mN/m, when a sufficient amount of effective lung surfactant is spread or adsorbed at the air−liquid interface. This drop in surface tension is caused by the accumulation of surfactant phospholipids and proteins which adsorb to the air−liquid interface on contact to form an interfacial film, a spontaneous process likely driven by a large decrease in free energy.[26]

Upon addition of the surfactant/Au-NP suspension, the surface tension dropped immediately, i.e., within 5 s, from an initial value of 48 mN/m to a value near 27 mN/m, indicating the formation of a surface-active film (see Figure 4a).

Postexpansion Adsorption Kinetics. The adsorption kinetics of surfactant material after rapid expansion of the interfacial film is shown in Figure 4b. It measures the ability of the expanding film to incorporate excess surfactant material which is associated with it, in the so-called surfactant reservoir, and maybe a better representation of the adsorption process as it actually occurs in the lung.[27] Here, we again observed a rapid surface tension drop, from a value near 35 mN/m just after expansion ($t = 0$) to below 27 mN/m within seconds indicating an active film.

Dynamic Compression/Expansion Isotherms. In the alveoli of the lung, minimum surface tension values near 0 are thought to occur during breathing and are essential in stabilizing the alveoli to collapse during end expiration.[18] In the CBS method, this property of the dynamic alveolar film is effectively reproduced: active surfactant films reach very low surface tensions without collapsing, when cycled dynamically.

The surface tension−area relation for dynamically cycled films is depicted in Figure 4c. As the interfacial film is compressed (area decrease) the surface molecules pack together more tightly, resulting in a significant drop in surface tension with the effect reversed upon expansion, as seen by the corresponding surface tension increase. After only a few cycles the films reached very low surface tensions (ca. 1 mN/m) with low compressibility, i.e., small area change and almost no hysteresis. The shape of the isotherms changed little even after 200 cycles.

Please note that there was a dramatic change in the curve shape observed during the first few cycles with the trend being to lower minimum surface tensions, smaller area changes, and disappearing curve hysteresis. This is a typical observation for films formed in the CBS and is likely the result of a progressive structural refinement of the surface film to a configuration which allows optimal packing of the surfactant film
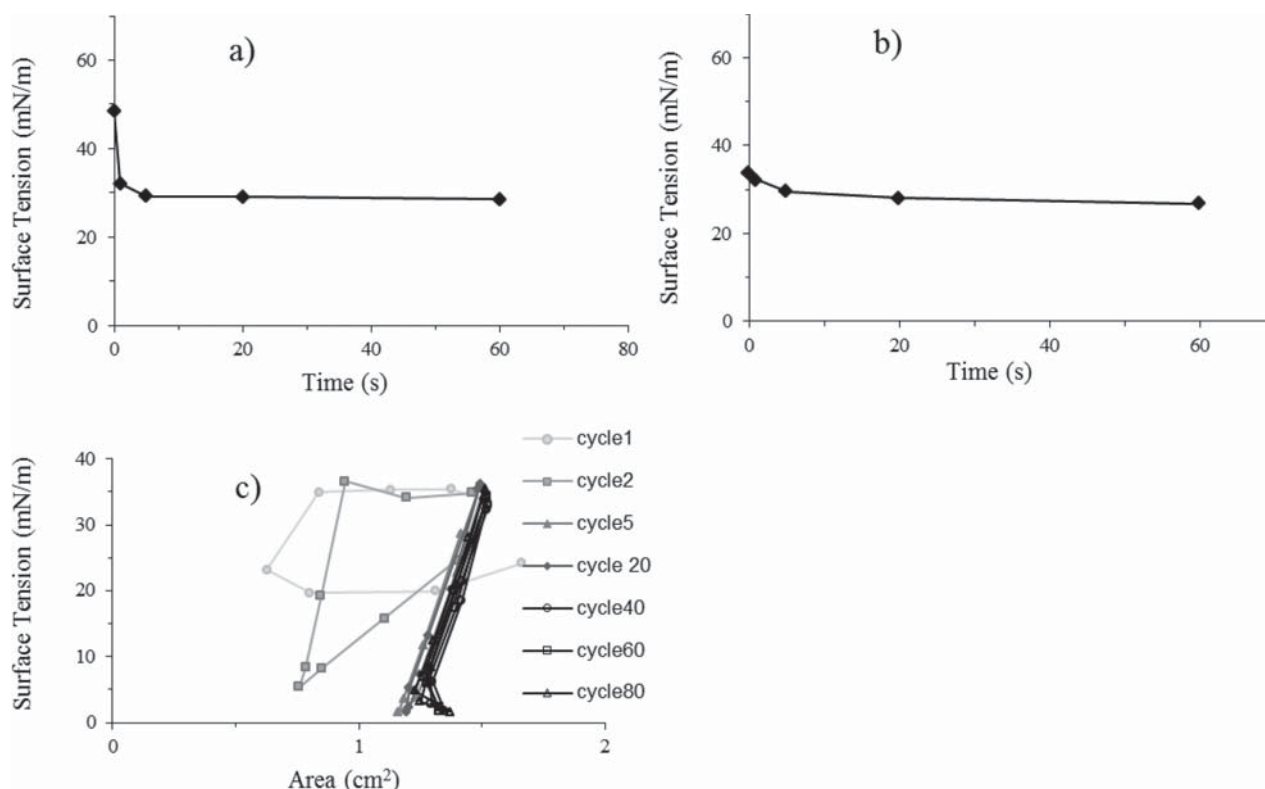
Figure 4. Biophysical characterization of interfacial film in CBS-cell method (representative experiment). (a) Adsorption kinetics (surface tension vs time) for film formed by injecting Au−NP−surfactant suspension (Au-NP, 40 nM, Curosurf, 20 mg/mL phospholipids) directly at air−liquid−cellular interface. The graph shows the drop in surface tension from the moment surfactant contacts the interface. (b) Postexpansion adsorption kinetics. The graph shows the drop in surface tension immediately after rapidly expanding the interfacial film. (c) Dynamic compression/expansion isotherms. The graph diplays the surface tension−area relation for continuous (dynamic) compression and expansion of the interfacial film. Shown are cycles 1, 2, 5, 20, 40, 60, and 80.

components.[27] The lack of hysteresis in the curves after several cycles is evidence for a very stable film; any structural collapse would cause molecules to be expelled from the interface, suddenly decreasing the area while leaving the surface tension largely unchanged. This would manifest as a distinct plateau in the isotherm and a large hysteresis.

Cell Viability in the CBS-Cell Model. Fluorescence microscope images (Figure 5a) show apoptotic (green) and corresponding necrotic (red) cells in epithelial lung cell layers either taken directly from the incubator (control) or integrated into the CBS system. The images are representative and reflect the statistical results (Figure 5b) for several independent experiments. Limited cell death was observed for both control and CBS-cell probes. Cell layers exposed to CBS-cell experimental conditions showed slightly more apoptosis and necrosis; however, overall differences were not statistically significant (Figure 5b).

Quantitation and Localization of Au-NPs inside Epithelial Lung Cells under Static and Dynamic Conditions. We carried out a number of experiments applying two different concentrations of Au-NPs, 40 and 28 nM in suspension with surfactant, to find the optimal concentration resulting in a detectable uptake into cells and hence facilitate their visualization and quantitation.

There were markedly more Au-NPs found inside the cells for experiments conducted at the higher concentrations (Supporting Information Figure S1). As a result, further experiments comparing cellular uptake of particles under static and dynamic conditions were done using the higher concentration of Au-

NPs in surfactant. With regard to Au-NP position in the cell layer, Figure 6a represents experiments under static and dynamic conditions. The *xy* and *xz* projection images, constructed from several optical sections, show the Au-NPs to be attached to the cell membrane (Figure 6a, static condition, arrow) or inside the cell (Figure 6a, dynamic condition, arrow).

Experiments carried out under dynamic conditions, yielded significantly more Au-NPs inside of the cells than those carried out under static conditions, as summarized in Figure 6b. Over a central area of 20 mm^2 of the cellular layer, at least 5 times more particle events were observed.

■ DISCUSSION

In this article we describe a new *in vitro* method modeling the alveolar epithelial barrier at the air−liquid interface under dynamic conditions. We were successful in fulfilling two key criteria: first, the formation of an active surfactant film at the air−liquid−cellular interface and, second, an epithelial lung cell layer integrated into the CBS in such a way that its viability was maintained for a full experimental protocol.

Interfacial films formed in the method were biophysically functional, exhibiting rapid film formation, low surface tensions, and low compressibility and stability (see Results section for details). In particular, very low minimum surface tensions, near 1 mN/m, were consistently reached during dynamic cycling: a key feature in mimicking the dynamic alveolar surface. It appears that neither the Au-NPs nor the A549 epithelial cell layer was detrimental to surfactant function. Furthermore, the
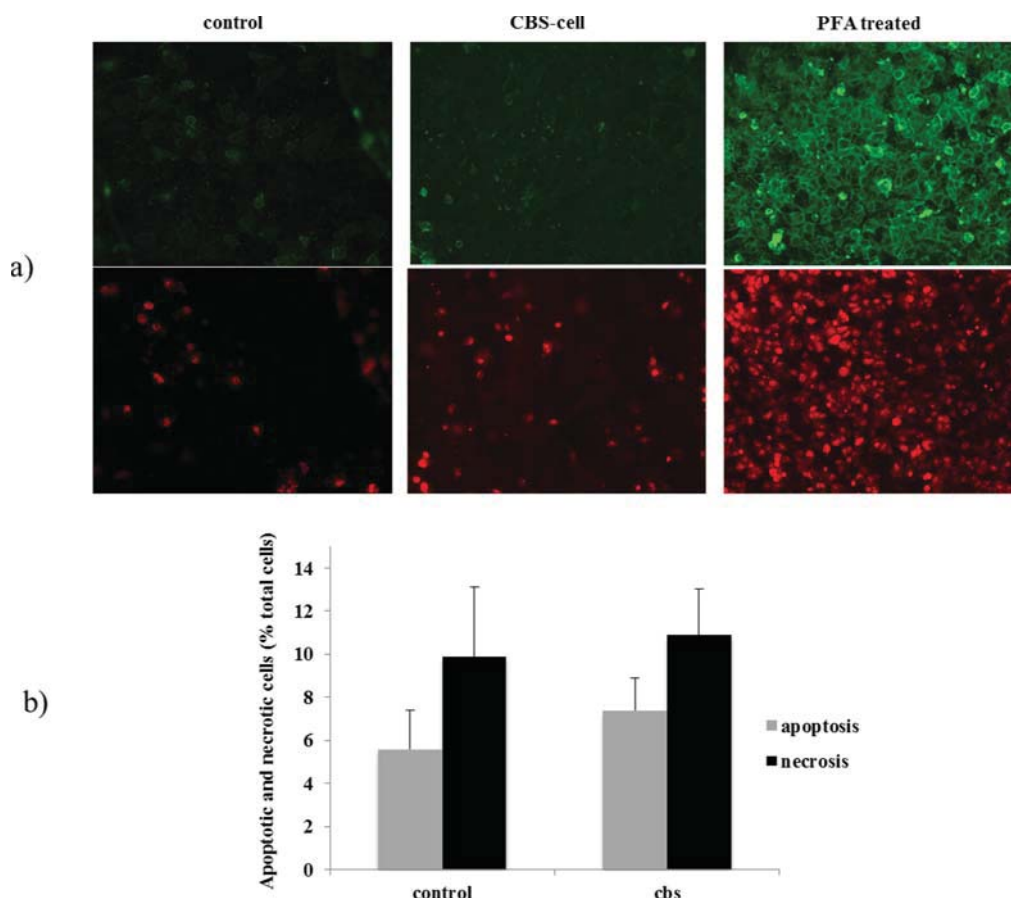
Figure 5. Cell viability assessment for CBS-cell method: (a) apoptotic (green) and necrotic (red) cells in A549 epithelial cell layer for control and CBS-cell experiments; (b) apoptosis/necrosis quantitation results compiled for at least four independent experiments.

A549 cells did not appear to be adversely affected by insertion into the CBS system and the subsequent dynamic conditions. Cell death was not significantly increased and the structural integrity of the cells also appeared intact. A549 cells are widely accepted as a model of human epithelial type II cells and produce surfactant when exposed to air.[28] In the CBS, the surfactant produced by these cells lowered the initial surface tension to 48 mN/m (vs ca. 72 mN/m for an air−water interface). We previously showed that when A549 cells are cultured at the air−liquid interface the surface tension drops down within 24 h to a value of 28 mN/m,[20] a value which had been measured *in vivo* in various animals. Since we could not culture the A549 cells in the CBS with a constant CO_2 supply, we decided to start the experiment immediately after inserting the cells into the system. Since the surfactant released from the cells did not adequately lower the surface tension, we knew it was not biophysically functional. Thus, we had to add an excess of Curosurf surfactant to form a functional film. The applied surfactant also served as convenient medium in delivering NP's to the air−liquid interface.

Satisfied with the functionality of the method, we investigated the influence of the dynamic interface on the uptake of Au-NPs by the underlying epithelial cell layer. We observed a highly significant effect on Au-NP uptake for experiments carried out under dynamic (breathing) conditions of compression and expansion of the air−liquid interface. The uptake of the particles was shown by LSM, revealing the intracellular localization in the A549 cells. We have already used the same particles and cells in a recently published study where

the quantification of intracellular Au-NPs by and their uptake mechanism was studied.[24] By using hybrid gold NPs with a fluorescent and an electron-dense moiety, the same particles can be evaluated by different quantitative microscopic techniques such as LSM and TEM. It was shown that by LSM events but not total numbers of intracellular fluorescently labeled NPs could be evaluated, while TEM gave quantitative numbers and more precise spatial information on intracellular NP localization, i.e., in vesicular structures. A predominant uptake via caveolin-mediated endocytosis was also found. However, the question if the same uptake mechanism applies for the dynamic breathing condition needs further investigation.

Another study using primary alveolar type II cells from rats and poly(ethylene glycol)-coated Au-NPs also showed uptake, but only very moderate;[29] these differences to our study might be explained by the different particle coatings and the different cell types used (primary vs cell line and human vs mice).

Perhaps more relevant to our study are the results obtained with the recently developed lung-on-a chip microdevice which models the alveolar−capillary barrier and allows for cyclical mechanical strain of the cellular interface to simulate breathing. They found a significantly higher uptake and translocation of NPs under cyclical mechanical strain compared to static conditions, results which were confirmed *in vivo*.[10]

While we did not apply a direct mechanical stretch to the cells, as in the above study, we did subject them to significant surface forces. It is possible that the changing surface tension is sensed by the underlying epithelial cells which could influence NP uptake. *In vivo*, surface forces at the air−liquid interface of
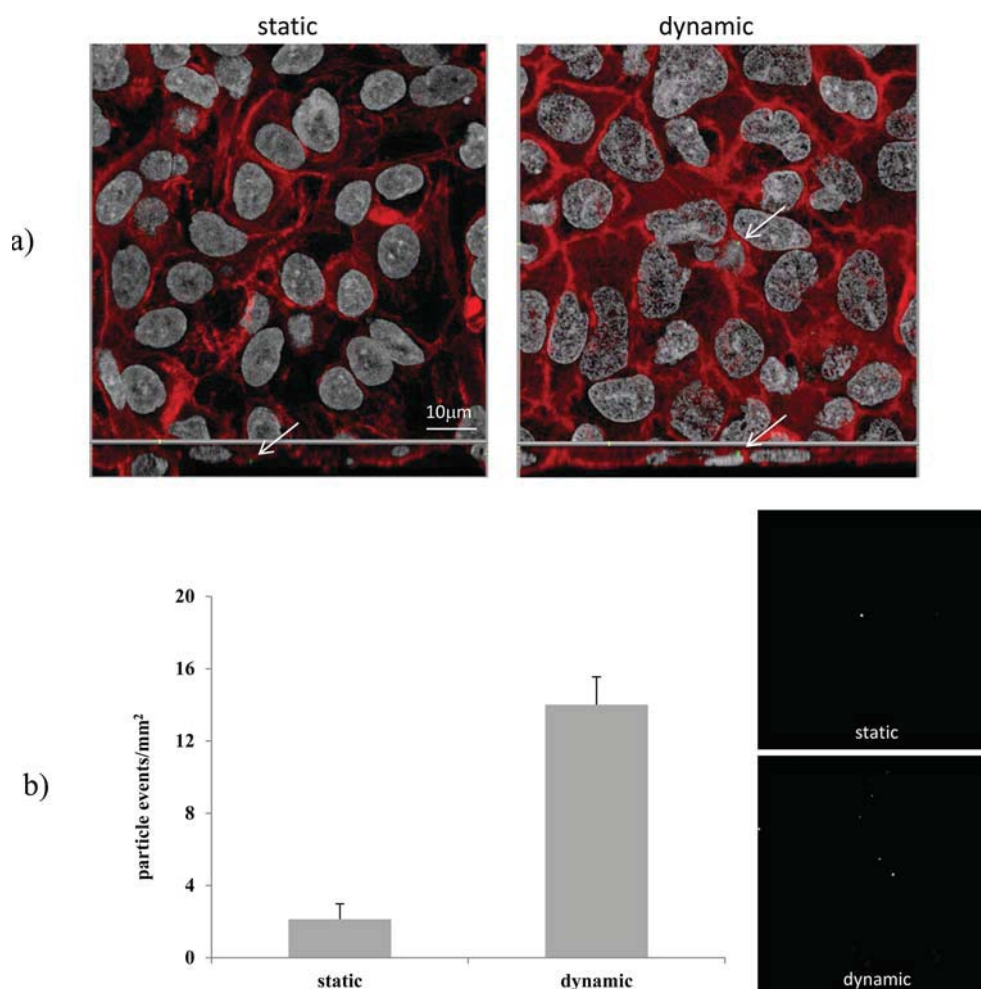
Figure 6. Visualization and quantification of Au-NPs in A549 epithelial cell layer with LSM. (a) Visualization of Au-NPs in epithelial cell layers with LSM. The F-actin cytoskeleton is shown in red, the cell nuclei in white, and the Au-NP fluorescence events appear as green points indicated by arrows. The representative images which include the top (*xy* plane) and sideview (*xz* plane) show the relative position of Au-NPs within the epithelial cell layer after CBS-cell experiments under static (left) and dynamic conditions (right). (b) Quantification of Au-NPs found in cells after CBS-cell experiments under static and dynamic conditions. The graph shows the results of a semiquantitative analysis of Au-NPs observed in the epithelial cell layer, as determined with LSM. The representative images (right) show the relative number of particle events found in the static and dynamic case within a defined area using a mean intensity of fluorescence projection. Results are based on four independent experiments.

the alveoli are significant and exert a molding effect on underlying tissue including epithelial cells.[30] Also supporting the argument of cellular sensing is a recent *in vitro* study where force applied to an air−liquid interface stimulated cellular response in underlying type II epithelial cells.[31] A follow-up study showed that an air−liquid interface containing a surfactant film acted as a stimulus to these same underlying cells.[32] Although conducted with different epithelial cells than in our study, these findings suggest that epithelial cells inserted into the CBS could be very sensitive to interfacial forces overlying them.

What other forces or factors associated with the dynamic interface could explain our results? Since the main physical feature of this interface is a rapidly changing surface tension, to near 0 values, it is sensible to question if this plays a role in facilitating NP displacement and subsequent cellular uptake. The displacement of NPs from the surfactant film at the surface could be faster at the very low surface tensions reached dynamically (see Introduction) and could promote direct interaction with the surface of epithelial cells. Previous *in vitro* and *in vivo* results, using aerosol deposition of particles, show that lower surface tensions and smaller particle size both favor particle wetting and immersion below the air−liquid interfacial film.[13] However, since we did not deposit NPs directly from the air, but rather applied them in suspension with surfactant, it is probable that many of the NPs were already completely wetted/immersed before application to the interface. Therefore, the above wetting argument may not be adequate in explaining the far greater number of NP's taken up under dynamic conditions. We surmise that NPs, completely immersed below the surface of the interfacial film, could be further displaced toward the underlying cells by the mechanical action of compression and expansion of said film. Further experiments are needed to clarify this point.

■ CONCLUSION

The CBS with integrated epithelial lung cells seeks to model the alveolar epithelial barrier of the lung *in vitro*. While it does not closely resemble the complex structure and mechanics of the breathing lung surface, to the best of our knowledge it does provide realistic surface tension dynamics at the air−liquid interface of human epithelial lung cells *in vitro*. Early results

investigating particle uptake under dynamic interfacial conditions are consistent with recent *in vivo* findings[10] and suggest the method to be an important tool for the *in vitro* study of NP-surfactant/NP-cell interactions under dynamic, i.e. breathing, conditions.

■ ASSOCIATED CONTENT

⑤ Supporting Information
Experimental data on expansion adsorption kinetics (Table S1), dynamic cycling data for the CBS-cell experiments (Table S2), visualization of Au-NPs in epithelial cells by LSM (Figure S1), and a video showing the compression/expansion of the air–liquid interface.

■ AUTHOR INFORMATION

Corresponding Author
*Phone +41 26 300 95 02; e-mail barbara.rothen@unifr.ch (B.R.-R.).

Notes
The authors declare no competing financial interest.

■ ACKNOWLEDGMENTS

■ REFERENCES

(1) Heyder, J.; Rudolf, G.; Schiller, C.; Stahlhofen, W. Deposition of particles in the human respiratory tract in the size range 0.005–15 μm. *J. Aerosol Sci.* **1986**, *17*, 811–825.

(2) Patton, J. S.; Byron, P. R. Inhaling medicines: delivering drugs to the body through the lungs. *Nat. Rev. Drug Discovery* **2007**, *6*, 67–74.

(3) Oberdorster, G.; Oberdorster, E.; Oberdorster, J. Nanotoxicology: an emerging discipline evolving from studies of ultrafine particles. *Environ. Health Perspect.* **2005**, *113*, 823–839.

(4) Gehr, P.; Schürch, S.; Berthiaume, Y.; Im Hof, V.; Geiser, M. Particle retention in airways by surfactant. *J. Aerosol Med.* **1990**, *3*, 27–43.

(5) Ochs, M.; Weibel, E. Functional design of the human lung for gas exchange. *Fishman' Pulmonary Diseases and Disorders*, 4th ed.; McGraw-Hill: New York, 2008.

(6) Kilburn, K. H. A hypothesis for pulmonary clearance and its implications. *Am. Rev. Respir. Dis.* **1968**, *98*, 449–63.

(7) De Jong, W. H.; Borm, P.-J. A. Drug delivery and nanoparticles: Applications and hazards. *Int. J. Nanomed.* **2008**, *3*, 133–149.

(8) Mansour, H. M.; Rhee, Y.-S.; Wu, X. Nanomedicine in pulmonary delivery. *Int. J. Nanomed.* **2009**, *4*, 299–319.

(9) Rothen-Rutishauser, B.; Kiama, S. G.; Gehr, P. A three-dimensional cellular model of the human respiratory tract to study the interaction with particles. *Am. J. Respir. Cell Mol. Biol.* **2005**, *32*, 281–289.

(10) Huh, D.; Matthews, B. D.; Mammoto, A.; Montoya-Zavala, M.; Hsin, H. Y.; Ingber, D. E. Reconstituting organ-level lung functions on a chip. *Science* **2010**, *328*, 1662–1668.

(11) Huh, D.; Leslie, D. C.; Matthews, B. D.; Fraser, J. P.; Jurek, S.; Hamilton, G. A.; Thornelowe, K. S.; McAlexander, M. A.; Ingber, D. E. A human disease model of drug toxicity-induced pulmonary edema in a lung-on-a-chip microdevice. *Sci. Transl. Med.* **2012**, *4*, 159ra47.

(12) Gil, J. W.; Weibel, E. R. Extracellular lining of bronchioles after perfusion-fixation of rat lungs for electron microscopy. *Anat. Rec.* **1971**, *169*, 185–199.

(13) Schürch, S.; Gehr, P.; Im Hof, V.; Geiser, M.; Green, F. Surfactant displaces particles toward the epithelium in airways and alveoli. *Respir. Physiol.* **1990**, *80*, 17–32.

(14) Schleh, C.; Kreyling, W. G.; Lehr, C.-M. Pulmonary surfactant is indispensable in order to simulate the in vivo situation. *Part. Fibre Toxicol.* **2013**, 10.

(15) Schürch, S.; Bachofen, H.; Goerke, J.; Possmayer, F. A captive bubble method reproduces the in situ behavior of lung surfactant monolayers. *J. Appl. Physiol.* **1989**, *67*, 2389–2396.

(16) Schoel, W. M.; Schürch, S.; Goerke, J. The captive bubble method for the evaluation of pulmonary surfactant: surface tension, area, and volume calculations. *Biochim. Biophy. Acta.* **1994**, *1200*, 281–290.

(17) Schürch, S.; Goerke, J.; Clements, J. A. Direct determination of surface tension in the lung. *Proc. Natl. Acad. Sci. U. S. A.* **1976**, *73*, 4698–4702.

(18) Bachofen, H.; Schürch, S.; Urbinelli, M.; Weibel, E. R. Relations among alveolar surface tension, surface area, volume, and recoil pressure. *J. Appl. Physiol.* **1987**, *62*, 1878–1887.

(19) Lieber, M.; Todaro, G.; Smith, B.; Szakal, A.; Nelson-Rees, W. A continuous tumor-cell line from a human lung carcinoma with properties of type II alveolar epithelial cells. *Int. J. Cancer* **1976**, *17*, 62–70.

(20) Blank, F.; Rothen-Rutishauser, B. M.; Schürch, S.; Gehr, P. An optimized in vitro model of the respiratory tract wall to study particle cell interactions. *J. Aerosol Med.* **2006**, *19*, 392–405.

(21) Shukla, R.; Bansal, V.; Chaudhary, M.; Basu, A.; Bhonde, R. R. Biocompatibility of gold nanoparticles and their endocytotic fate inside the cellular compartment: A microscopic overview. *Langmuir* **2005**, *21*, 10644–10654.

(22) Lin, C. A. J.; Sperling, R. A.; Li, J. K.; Yang, T. Y.; Li, P. Y.; Zanella, M.; Chang, W. H.; Parak, W. J. Design of an amphiphilic polymer for nanoparticle coating and functionalization. *Small* **2008**, *4*, 334–341.

(23) Mahmoudi, M.; Abdelmonem, A. M.; Behzadi, S.; Clement, J. H.; Dutz, S.; Ejtehadi, M. R.; Hartmann, R.; Kantner, K.; Linne, U.; Maffre, P.; Metzler, S.; Moghadam, M. K.; Pfeiffer, C.; Rezaei, M.; Ruiz-Lozano, P.; Serpooshan, V.; Shokrgozar, M. A.; Nienhaus, G. U.; Parak, W. J. Temperature: the "ignored" factor at the NanoBio interface. *ACS Nano* **2013**, *7*, 6555–6562.

(24) Rothen-Rutishauser, B.; Kuhn, D. A.; Ali, Z.; Gasser, M.; Amin, F.; Parak, W. J.; Vanhecke, D.; Fink, A.; Gehr, P.; Brandenberger, C. Quantification of gold nanoparticle cell uptake under controlled biological conditions and adequate resolution. *Nanomedicine* **2013**, in press.

(25) Schürch, S.; Bachofen, H.; Possmayer, F. Surface activity in situ, in vivo, and in the captive bubble surfactometer. *Comp. Biochem. Physiol., Part A: Mol. Integr. Physiol.* **2001**, *129*, 195–207.

(26) Schürch, S.; Green, F. H.; Bachofen, H. Formation and structure of surface films: captive bubble surfactometry. *Biochim. Biophys. Acta* **1998**, *1408*, 180–202.

(27) Schürch, D.; Ospina, O. L.; Cruz, A.; Perez-Gil, J. Combined and independent action of proteins SP-B and SP-C in the surface behavior and mechanical stability of pulmonary surfactant films. *Biophys. J.* **2010**, *99*, 3290–3299.

(28) Muñoz, J. L. Study of surfactant secretion in the A549 cell line: A tissue culture model for the type II pneumocyte, Yale University, 1978.

(29) Bouzas, V.; Haller, T.; Hobi, N.; Felder, E.; Pastoriza-Santos, I.; Perez-Gil, J. Nontoxic impact of PEG-coated gold nanospheres on functional pulmonary surfactant-secreting alveolar type II cells. *Nanotoxicology* **2014**, *8*, 813–823.

(30) Bachofen, H.; Schürch, S. Alveolar surface forces and lung architecture. *Comp. Biochem. Physiol., Part A: Mol. Integr. Physiol.* **2001**, *129*, 183−93.

(31) Ravasio, A.; Hobi, N.; Bertocchi, C.; Jesacher, A.; Dietl, P.; Haller, T. Interfacial sensing by alveolar type II cells: a new concept in lung physiology? *Am. J. Physiol. Cell Physiol.* **2011**, *300*, 456−465.

(32) Hobi, N.; Ravasio, A.; Haller, T. Interfacial stress affects rat alveolar type II cell signaling and gene expression. *Am. J. Physiol. Lung Cell Mol. Physiol.* **2012**, *303*, 117−129.